NURETH-331

EXPERIMENTAL INVESTIGATIONS ON THE STEADY STATE AND STABILITY BEHAVIOR OF SUPERCRITICAL PRESSURE NATURAL CIRCULATION

P.K. Vijayan¹, S.B. Thakuria², M. Sharma¹, D.S. Pilkhwal¹, D.Saha¹ and R.K. Sinha¹ Reactor Engineering Division, Bhabha Atomic Research Centre, Mumbai, India

²Homi Bhabha National Institute, Mumbai, India

Abstract

Natural circulation experiments were carried out in a uniform diameter rectangular loop using supercritical CO₂ and H₂O. Steady state data were generated with supercritical CO₂ with four different orientations of the source and sink. Instability was observed only for the orientation with both the source and sink horizontal over a narrow window of power around the pseudocritical point with low cooling water flow rate. Hence experiments with water were carried out only for this orientation which also showed instability at low coolant flow rates. The steady state flow rates obtained were compared with a generalized flow correlation developed which showed good agreement with present data as well as those reported in literature. The general characteristics of the observed instability are also described in the paper.

Keywords: Supercritical fluids, natural circulation, steady state and instability behaviour

Introduction

Thermodynamically supercritical fluids are one of the several coolant options being investigated currently for advanced nuclear reactors. Both supercritical CO₂ [1,2] and supercritical water [3-6] are candidate coolants for advanced reactors. The main advantage of supercritical fluids is higher thermodynamic efficiency due to the larger operating temperature. Since boiling is avoided, the critical heat flux phenomenon is eliminated raising the possibility of higher power density. Besides supercritical fluids like water can be directly sent to the turbine eliminating the requirement of steam generator, steam-water separator, dryer and pressurizer. Further, most supercritical reactor designs proposed are once-through type reducing the number of components like pumps. In addition, components like feed water pumps are of significantly lower rating compared to their counterparts in the current LWRs of same rating due to the significantly larger enthalpy rise across the core. The higher power density could significantly lower the core size and hence the vessel size. The foregoing advantages suggest that the supercritical reactor could be far more competitive economically compared to the current LWRs.

However, the supercritical fluids undergo significant property changes in the pseudo-critical region. For example, the density changes in supercritical reactors are comparable to or more than that in present day BWRs raising the possibility of density wave instability. In view of this, several investigators [7-8] have already looked at the instability of supercritical fluids. A few investigations were also conducted with supercritical CO₂ which is a good simulant fluid for water [9-11]. Fluid-to-fluid modeling aspects have been studied by Marcel et al. [12] and found

that a 77.5%/22.5% mixture of refrigerants R-32 & R-125 simulates the supercritical water (SCW) conditions in HPLWR (High Performance Light Water Reactor). They also found that supercritical CO₂ cannot accurately simulate the HPLWR conditions with water. In a more recent study by the same group Rohde et al. [13], R23 has been proposed as the scaling fluid it has more convenient substance properties and is safer to operate. A few studies have been made to extend the generalized dimensionless parameters applicable for stability analysis of two-phase flows to supercritical fluids [14-15]. Some of these studies were carried out in natural circulation systems [9-11 & 16] as it is also a possible option for supercritical reactors [17-18]. However, very few experimental studies are reported in the open literature. Lomperski et al. [19] reported steady state natural circulation data in a rectangular loop with supercritical CO₂ but did not observe instability. Holman-Boggs [20] reported only steady state data with supercritical Freon-12 although they had observed instability. Harden [21] reported both steady state and instability data with supercritical Freon-114. Besides Yoshikawa et al. [22] studied the performance of a somewhat complex supercritical CO2 loop. Although instability has been reported for supercritical fluids by many authors [20, 21 & 23], to our knowledge, the instability characteristics of supercritical fluids are not studied in detail. In this context an experimental investigation of the steady state and stability behavior has been carried out in a uniform diameter rectangular natural circulation loop with supercritical CO₂ and water as the working fluids. The experiments with supercritical CO₂ were carried out with four different loop configurations. Instability, however, was observed only for the loop with horizontal heater and horizontal cooler at low secondary coolant flow rates over a narrow window of power around the pseudocritical point. Hence experiments were repeated with water for the horizontal heater and horizontal cooler configuration only. Instability was also observed at low secondary coolant flow rate with water around the pseudocritical point. The general characteristics of the observed instability are described in the paper and a mechanism for the instability is also proposed. The steady state and stability data generated were analyzed using 1-D theory. The results have also been compared with that of previously reported studies.

Description of the test facility

The test facility is a uniform diameter (13.88 mm inside diameter (ID) & 21.34 mm outside diameter (OD)) rectangular loop made of type-347 stainless steel. Standard 41.4 MPa (6000 lb) rating socket weld type elbows are used at the corners. The loop has two heater and two cooler sections so that it can be operated in any one of the four orientations such as Horizontal Heater Horizontal Cooler (HHHC), Horizontal Heater Vertical Cooler (HHVC), Vertical Heater Horizontal Cooler (VHHC) and Vertical Heater Vertical Cooler (VHVC). The heater was made by uniformly winding nichrome wire over a layer of fiber glass insulation. The cooler was tube-in-tube type with chilled water as the secondary coolant flowing in the annulus. The outer tube forming the annulus had 77.9 mm ID and 88.9 mm OD. The loop had a pressuriser located at the highest elevation which takes care of the thermal expansion besides accommodating the cover gas helium above the carbon dioxide. The safety devices of the loop (i.e. rupture discs RD-1 & RD-2) were installed on top of the pressuriser which also had provision for CO₂ & He filling. The entire loop was insulated with three inches of ceramic mat (k=0.06 W/mK).

The loop was instrumented with 44 calibrated K-type mineral insulated thermocouples (1 mm diameter) to measure the primary fluid, secondary fluid and heater outside wall temperatures. Primary fluid temperatures at each location was measured as the average value indicated by two thermocouples inserted diametrically opposite at r/2 (see detail-D in Fig. 1) from the inside wall whereas secondary fluid temperatures were measured by a single thermocouple located at the tube centre of the inlet and outlet nozzles (see thermocouples T41 to T44 in Fig. 1). This was adequate to obtain the average temperature as the temperature rise in the secondary fluid was small (< 4 °C). The thermocouples used to measure the heater outside wall temperature (two thermocouples installed diametrically opposite at six axial locations) were installed flush with the outside surface. The system pressure was measured with the help of two Kellar make pressure transducers located on the pressuriser as well as at the vertical heater outlet. The pressure drop across the bottom horizontal tube (see detail-B) and the level in the pressuriser were measured with the help of two differential pressure transmitters. The power of each heater was measured with a Wattmeter. The secondary flow rate was measured with the help of a turbine flow meter. All instruments were connected to a data logger with a user selectable scanning rate. For all the transient and stability tests the selected scanning rate was 1 second.

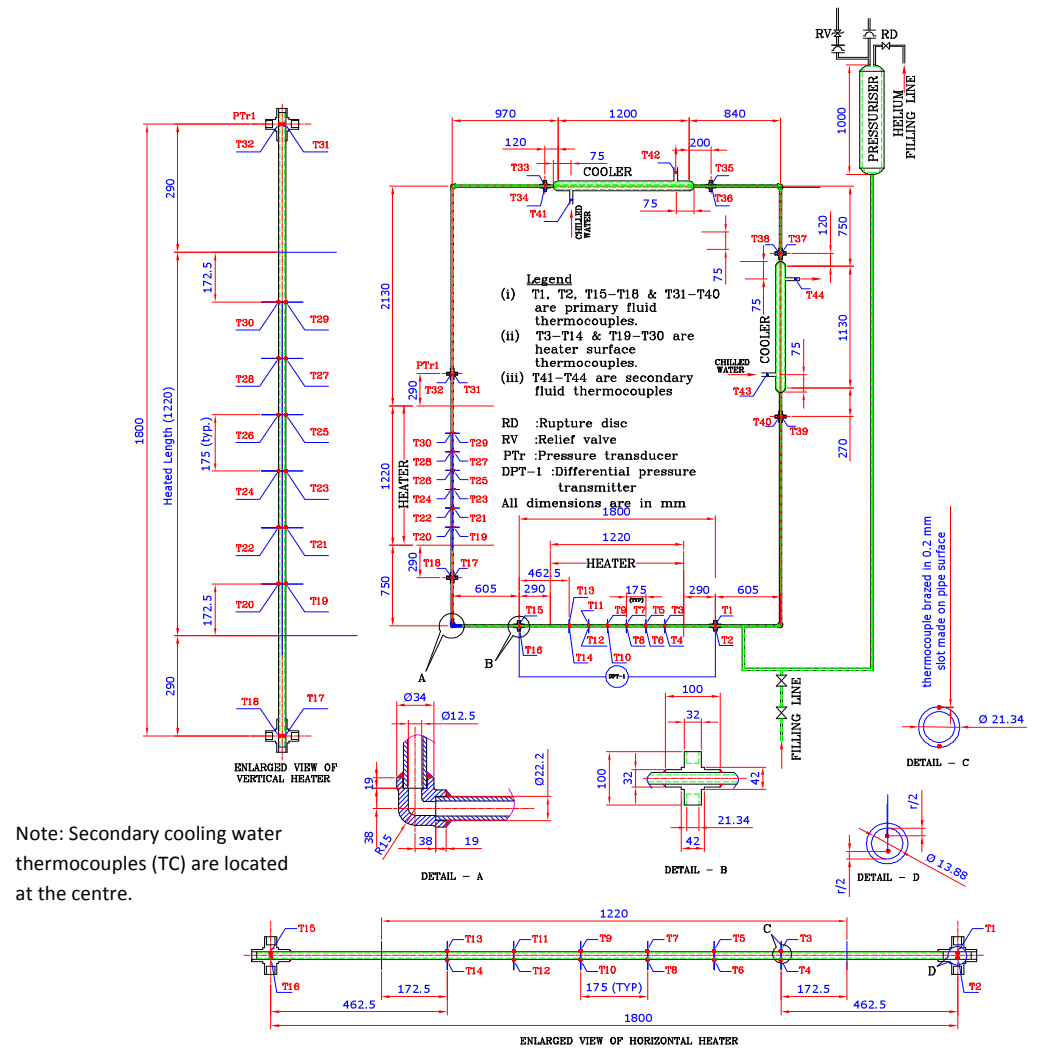


Fig. 1: Supercritical pressure natural circulation loop (SPNCL)

The accuracy of the thermocouples were within \pm 1.5 0 C. The accuracy of the pressure and differential pressure measurements were respectively \pm 0.3 bar and \pm 0.18 mm. The accuracy of the secondary flow as well as power measurements were \pm 0.5 % of the reading. In addition, typical fluctuations of each instrument were also recorded during steady state with and without power which was practically same. Maximum fluctuation in primary temperature, secondary temperature, loop pressure and pressure drop were respectively \pm 0.44 0 C, \pm 0.1 0 C, \pm 0.28 bar and \pm 0.21 mm.

Shakedown Tests

The purpose of the shakedown tests was to generate heat loss and pressure drop characteristics of the loop. The pressure drop characterization tests were carried out under forced flow conditions in a separate facility. The pressure drop data for the loop piping and the loss coefficient data for the elbows are plotted in Fig. 2. The measured friction factor was somewhat larger than that for smooth pipes due to the use of commercial pipes. The correlations fitted to the friction factor and loss coefficient data are also shown in Fig. 2. To estimate the heat losses, natural circulation experiments were carried out at various powers with water at subcritical conditions (Fig.3). Adequacy of the loop instrumentation for estimating the mass flow rate was also tested during these experiments [24].

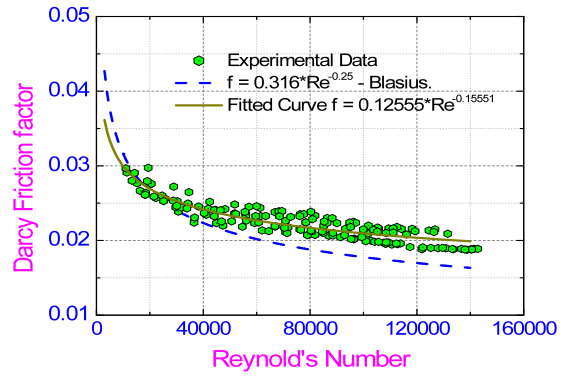
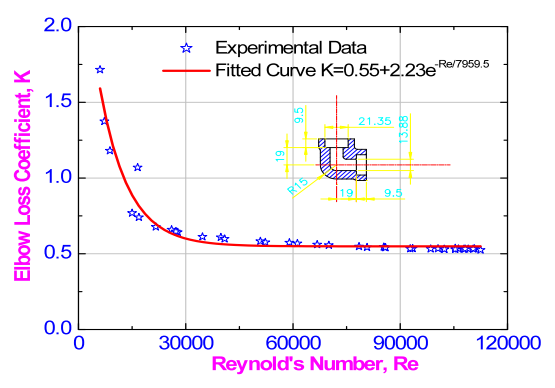


Fig. 2a: Friction factor data for the tube used in the construction of the loop



Fig, 2b: Loss coefficient data for the 90° elbow used in the loop

Experiments with supercritical CO₂

Before operation with supercritical CO₂, the loop was flushed repeatedly with CO₂ at low pressure including all impulse, drain and vent lines. Subsequently the loop was filled with CO₂ up to 50 bar pressure and the chilled water coolant was valved in. This caused condensation of CO₂ and hence a decrease in loop pressure. The pressure decrease was compensated by admitting additional CO₂ from the cylinder and again allowed sufficient time for condensation. The process of filling and condensation was continued till there was no decrease in pressure. At this point the loop pressure was increased to the required value with the help of a helium gas cylinder. Once the required supercritical pressure was achieved, the helium cylinder was isolated from the pressuriser. Sufficient time was allowed to reach steady state. However, it was found difficult to attain completely stagnant conditions with uniform temperature throughout the loop as the higher ambient temperature allowed small amount of heat absorption through the insulation into the

loop which was rejected at the cooler causing a small circulation rate. Once a steady state was achieved, the heater power was switched on and adjusted to the required value. Sufficient time was allowed to achieve the steady state. Once the steady state is achieved, power was increased and again sufficient time was provided to achieve the steady state. In case the system pressure increases beyond the set value by 1 bar, a little helium was vented out to bring back the pressure to the original value. Similarly during power decrease if the pressure decreases below the set point by one bar, then the loop was pressurized by admitting additional helium into the pressurizer. The experiments were repeated for different pressures and different chilled water flow rates. Subsequently the experiments were performed for different orientations of the heater and cooler.

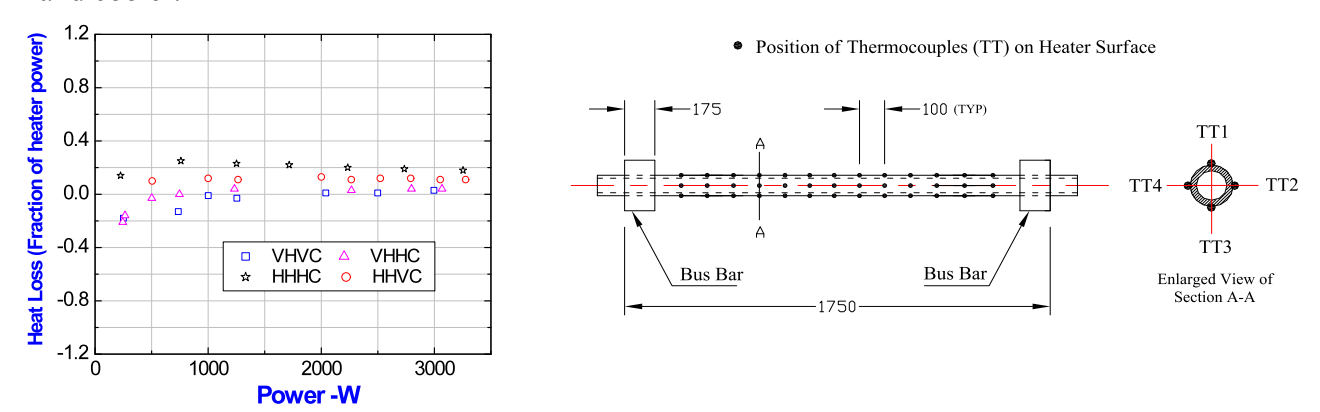


Fig. 3: Estimated heat loss fraction for various orientations during subcritical NC tests with water

Fig. 4: Inconel-625 heater test section for Supercritical water loop

Facility for operation with supercritical water

After completion of experiments with CO₂, the supercritical pressure natural circulation loop (SPNCL) was modified by installing new test sections, pressurizer (designed for 30 MPa), Haskel pump and a low voltage high current power supply (25V & 8000A rated 200kW) so that uniform heat generation occurs in the heater wall material. The pressuriser with provision for gas filling (nitrogen) and the safety devices (rupture discs) was connected to the main loop as shown in Fig. 5. The cooler is the same as in CO₂ loop albeit cooled with air using a large capacity blower (i.e. 45,300 lpm at 20 m head). Besides, the heater instrumentation and the secondary system flow measurement of the loop were also modified. Thermocouples were brazed on the outside surface of each heater test section, at twelve different axial locations. At each location, four thermocouples were provided at 90° angular distance (each at top, bottom and sides) as shown in Fig. 4. A total of 124 thermocouples were installed in the water loop compared to 44 thermocouples in the CO₂ loop. This also necessitated the use of a new data logger. An anubar was used for the air flow measurement. As fabricated length scales of the modified SPNCL are given in Fig. 5.

Experiments with Supercritical Water

For experiments under supercritical pressure conditions with water the following operating procedure is followed:

- i) The loop is filled up with demineralised water to the required level in the pressurizer.
- ii) Nitrogen is filled at the top of the pressurizer and the loop pressure is increased to 11 MPa.
- iii) Further pressurization to 22 MPa and beyond is achieved by injecting more water at the bottom of the pressurizer with the Haskel pump which increases the water level in the pressurizer. Then the Haskell pump is isolated.
- iv) Now power is switched on and due to thermal expansion of water, the loop gets pressurized above the supercritical pressure.
- v) To get desired pressure at an operating power, water inventory in the pressurizer is changed by either injecting water with Haskel pump or draining water from drain line near the outlet of Haskel pump.

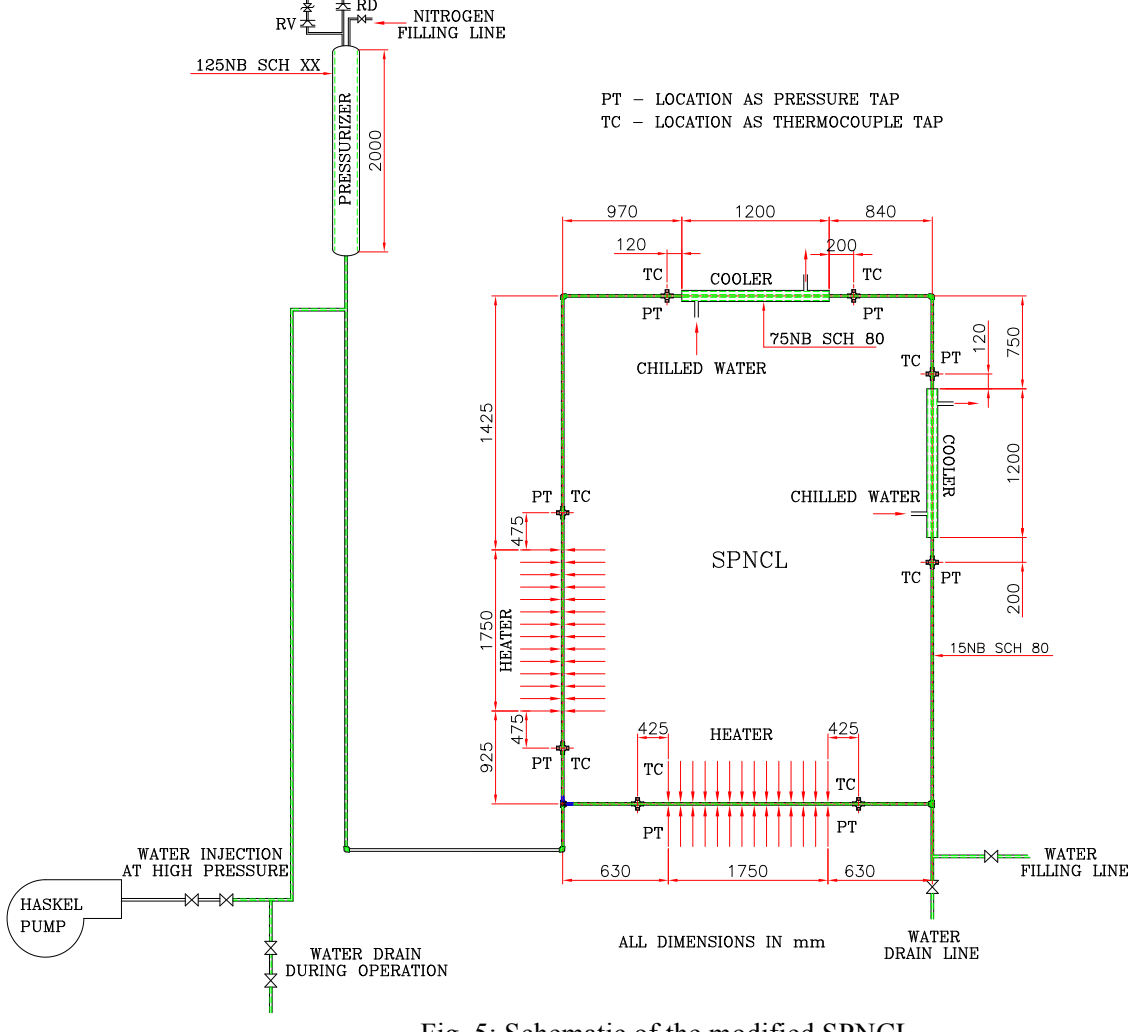


Fig. 5: Schematic of the modified SPNCL

Steady State Data

Steady state data on natural circulation flow rate were generated with supercritical CO₂ for various orientations of the source and sink whereas data with supercritical water was generated

only for the orientation with both the source and sink horizontal. The range of parameters of all the steady state data for CO₂ and water is given in table-1.

The steady state mass flow rate for the experimental conditions were estimated using the measured heater power and the enthalpy rise across the heater as

$$W = \frac{Q_h}{i_{ho} - i_{hi}} \tag{1}$$

Table-1: Range of parameters for steady state natural circulation data with CO₂ and water

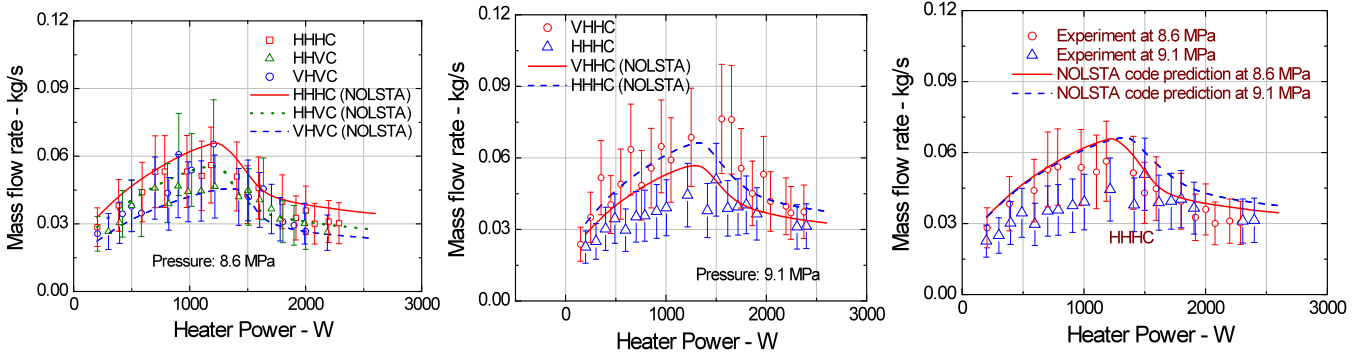
Supercr	itical carbon dioxide data	Supercritical water data			
Variables	Range	Variables	Range		
Orientation	HHHC, HHVC, VHHC & VHVC	Orientation	HHHC only		
Pressure	8-9.2 MPa	Pressure	22.4-24.1 MPa		
Power	0.1-2.4 kW	Power	3.5-8 kW		
Coolant	Chilled water	Coolant	air		
Cold leg temp.	17.5-57.7 °C	Cold leg temperature	207 – 403 °C		
Hot leg temp.	19.3-95.9 °C	Hot leg temperature	199 - 424 °C		
Coolant flow	29.6-56 lpm (liters per minute)	Coolant flow	7712 – 14617 lpm		
Coolant inlet	8.2-11.4 °C	Coolant inlet	44.3 – 46.5 °C		
Coolant outlet	9.0-12.5 °C	Coolant outlet	71.6 – 93 °C		

The enthalpies at the heater inlet and outlet were estimated using the corresponding measured temperatures and system pressure. This is a better approach to estimate the experimental flow rate since the specific heat variation is significant for supercritical fluids. The estimated flow rates were compared with the predictions of the in-house developed computer code NOLSTA [25] and the results are presented in Fig. 6a & b. Figure 6a shows the data for three different orientations for which data were available at 8.6 MPa. For the VHHC orientation data were available only for 9.1 MPa. The data for VHHC and HHHC orientations are compared with NOLSTA predictions in Fig. 6b. The data are found to be in reasonable agreement with the code predictions. The effect of pressure on the steady state flow rate is presented in Fig. 6c along with the predictions by the NOLSTA code. The experimental steady state mass flow rate, heater inlet and outlet temperatures versus power for supercritical water at constant secondary side air flow rate are shown in Fig. 7a & b respectively. The predictions by NOLSTA code are in close agreement with experimental data.

A generalized steady state flow equation has been derived by Swapnalee et al. [26] based on the dimensionless property relationship given by Ambrosini and Sharabi [27, 28]. According to Swapnalee et al. [26] the supercritical region can be subdivided in to various regimes as shown in figure 8a. The equation given for region 2 (where majority of the steady state data from the present tests belong) is reproduced below

$$Re = 1.907 \left(\frac{Gr_m}{N_G} \right)^{0.364}$$
 (2)

The above dimensionless flow equation is compared with the present steady state supercritical pressure natural circulation flow data for CO_2 and water in Fig. 8b. Subsequently, the data reported by Lomperski et al [19], Harden [20] and Holman-Boggs [21] are also compared with the above equation in Fig. 8c. In all cases, reasonable agreement is obtained with the proposed flow equation i.e. \pm 30%. Since the data is from four different supercritical fluids generated with nine different loop configurations, the above equation is expected to hold good for other supercritical fluids and loop geometries.



- (a) Steady state flow at 8.6 MPa
- (b) Steady state flow at 9.1 MPa
- (c) Pressure effect on steady state flow

Fig. 6 Measured and predicted steady state flow rate for various orientations

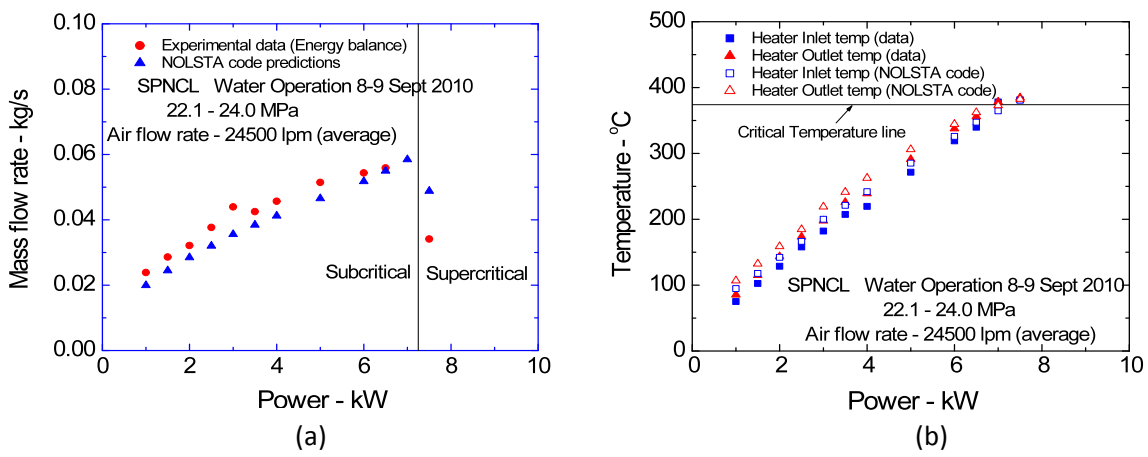
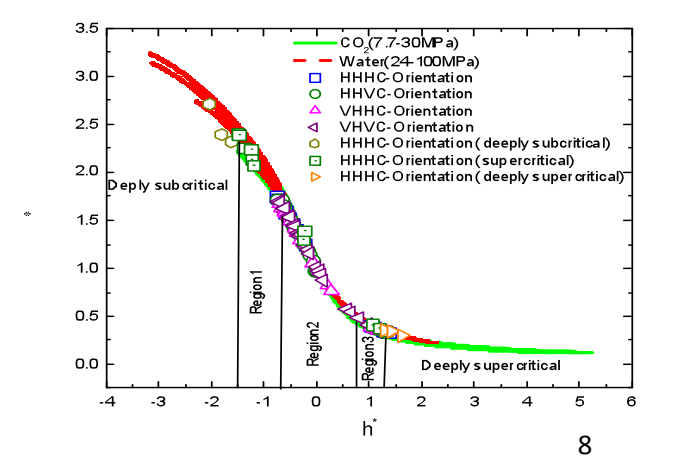
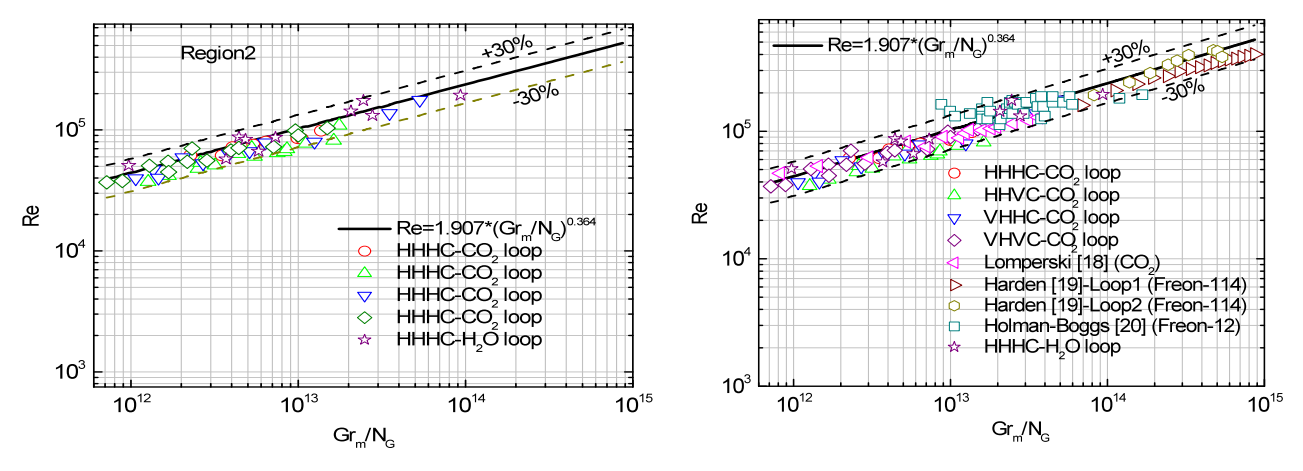


Fig. 7: Steady state flow rate data with supercritical water.



a) Classification of present SPNCL data in to various regions



b) Present data in dimensionless form

c) Steady state data from all loops

Fig. 8: Steady state natural circulation data compared with generalized equation

Stability Data

Instability was observed only for the HHHC orientation. All other orientations were fully stable. Even for the HHHC orientation, both the subcritical and the supercritical regions beyond the pseudo-critical region were found to be mostly stable. Instability was observed only for a narrow window in the pseudo-critical region at low secondary coolant flow rates. Table-2 lists all the instability data that was generated with supercritical CO₂. Instability was observed in the primary loop mass flow rate, heater outlet temperature and in some cases heater inlet temperature also during start-up from rest, power raising and step back from stable steady state.

Start-up from rest

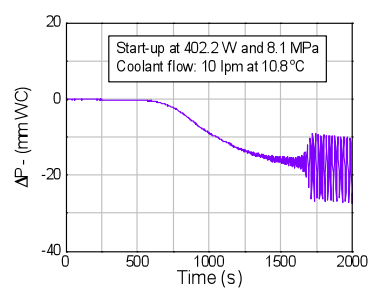
These tests were performed by switching on the power nearly 3 to 4 hours after valving in the chilled water flow. Since the ambient temperature (28-32 °C) was much above the coolant temperature (8.2-11.4 °C), complete stagnant conditions could not be achieved as explained earlier. Typical instabilities observed for start-up from rest are shown in Fig. 9. At 10 lpm flow, stable start-up is not observed in the clockwise flow direction for power greater than 200 W. Start-up tests were not performed below this power. However, analysis shows stable start-up at very low power. On the other hand if flow initiated in the counter-clockwise direction, it was found to be stable. Note that the loop is not completely symmetric (see Fig. 1). Table-2 shows a summary of the tests done i.e. Sr. no. 13, 15 and 17.

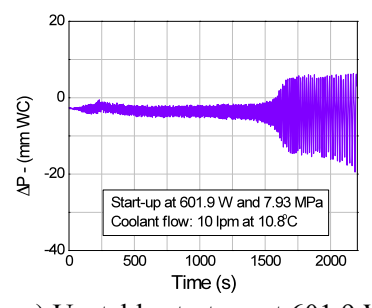
Power raised or lowered from stable steady state

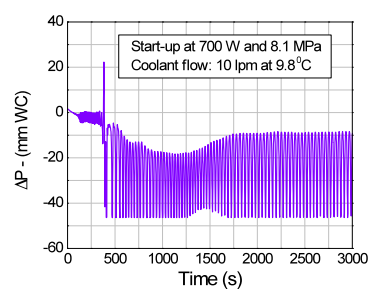
In this case, starting from a stable steady state the power is increased or decreased in small steps. These experiments were carried out at different pressures and secondary flow rates. Table-2 shows a summary of the tests done i.e. Sr. no. 1-3, 5-12 and 16.

Typical instability observed at 9.1 MPa at various powers is shown in Fig. 10, 11 and 12 respectively for different secondary flow rates of 10, 15 and 20 lpm. In all cases, the instability develops by the oscillation growth mechanism as proposed by Welander [29]. Instability

development from steady state condition by the oscillation growth mechanism was also observed in single-phase loops [30]. As seen from figures 10, 11 and 13, the instability dies by a steady decrease in oscillation amplitude. Instability was also observed at other pressures as shown in Fig. 13. In this case, a complex time series shows a complex oscillatory pattern with repetitive oscillation growth and decay.





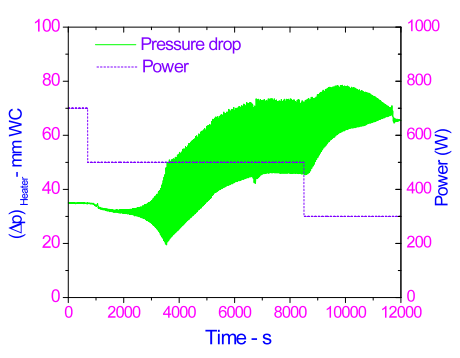


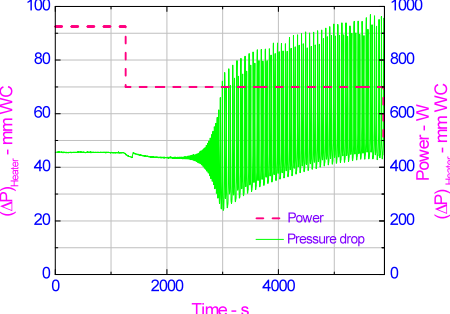
- a) Unstable start-up at 402.2 W
- c) Unstable start-up at 601.9 W
- d) Unstable start-up at 700 W

Fig. 9: Start-up from rest at different powers

Large power decrease from stable steady state:

Three tests are listed under this category in table-2 i.e. Sr. no. 4, 14, 18 and 19. In all cases the final power was the same and the initial power was different. Further the initial condition was stable and the final condition was unstable for all the cases (see Fig. 14).





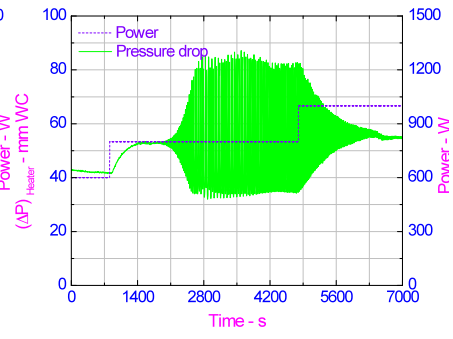


Fig. 10: Typical instability observed at 500 W and 9.1 MPa with 10 lpm coolant flow

a) Instability at 700 W

b) Instability at 800 W

Fig. 11: Instability observed at 9.1 MPa and 15 lpm coolant flow

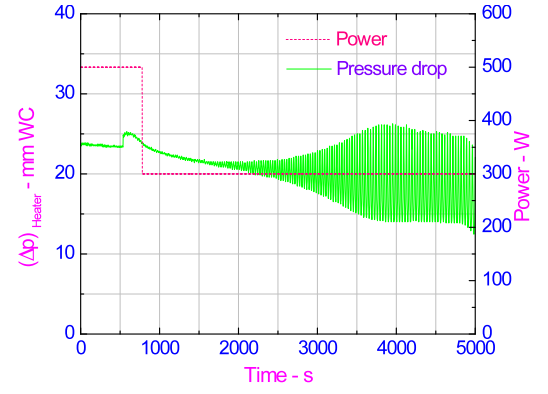


Fig. 12: Typical instability observed at 300 W and 9.1 MPa with 20 lpm secondary flow

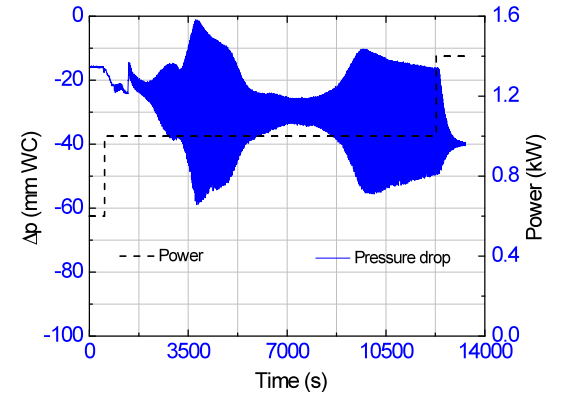


Fig. 13: Typical instability observed at 1000 W and 8.1 MPa with 10 lpm secondary flow

Table-2: Summary of instability data

Sr. no.	Data folder name	Date	P MPa	Power (W)	T _{hi} - °C	Tho - °C	T _{si} - °C	T _{so} - °C	W _s (lpm)	T _{PC} °C	Remarks
1	HHHC_90_15	12/6/09	9.1	198-400- 200	22.3- 34.2	30.3- 54.6	9.9	11	15.1	40	Only recorded graphs available
2	НННС_90_15	13/6/09	9.1	200-400- 600	25.5- 37.5	30- 58	9.9	11	15	40	Pressure raised at 3.20 hrs
3	HHHC_90_15	13/6/09	9.1	600-800- 1000	31	35- 43	9.8	10.9	15	40	
4	HHHC_90_15	13- 14/6/09	9.1	1692.73- 200- 1716.7	56	96.5- 99.7	10.3	11.1	15.1	40	Only recorded graphs available
5	НННС_90_15	14/6/09	9.1	925-700- 500	31	34- 45	9.8	11.2	15.5	40	
6	НННС_90_15	14/6/09	9.1	500-300- 100	45- 75	59- 111	9.8	10.7	15.1	40	At 9.50 temp reached 170 and then start falling
7	HHHC_90_10	14/6/09	9.1	Unknown- 200-400	40- 65	50- 100	10.2	11.6	10.2	40	Only recorded graphs available
8	HHHC_90_10	15/6/09	9.1	401.4- 579-790	30	65- 70	10.2	12	10.2	40	Only recorded graphs available
9	HHHC_90_10	15/6/09	9.1	700-500- 300	27.1	37- 45	9.8	11.4	10	40	
10	HHHC_90_10	15/6/09	9.1	300-100	16.7- 18.4	22.7- 25	10.3	11.2	10	40	
11	HHHC_90_20	16/6/09	9.1	500-300- 100	22	32- 35	9.5	10.5	20	40	
12	НННС_90_20	16- 17/6/09	9.1	300-100	16.2- 17	24.8- 26.5	9.6	10.4	20	40	
13	SR(3)_HHHC_ 400W_10	6/7/09	8.1	0-402.18	45.2- 76.1	52- 112.6	10.8	12.4	10	34.5	
14	SR(3)_HHHC_ 500W_10	7/7/09	8.1	1500-300	23- 25	28.1- 31.2	10.2	12	10	34.5	
15	SR(3)_HHHC_ 600W_10	8/7/09	7.93	0-601.87	31.5- 65	44- 92	10.8	11.6	10	33.5	High temperature trip at 10.07am
16	SR(4)_HHHC_ 600W_10	3/8/09	8.13	600-1000- 1400	30.6- 32.53	36.3- 38.9	9.2	10.4	10.1	35.5	
17	SR(4)_HHHC_ 700W_10	4/8/09	8.1	0-700W	29.4	31- 33	9.8	10.8	10	34.5	
18	SR(4)_HHHC_ 700W_10	4/8/09	7.7	1900-300	28.4	27- 34	9.1	9.9	10.2	32.5	
19	HHHC_500W _10_090809	9/8/09	8.1	1700-300	25.7- 26.2	27- 31	9.2	11.1	10.1	34.5	

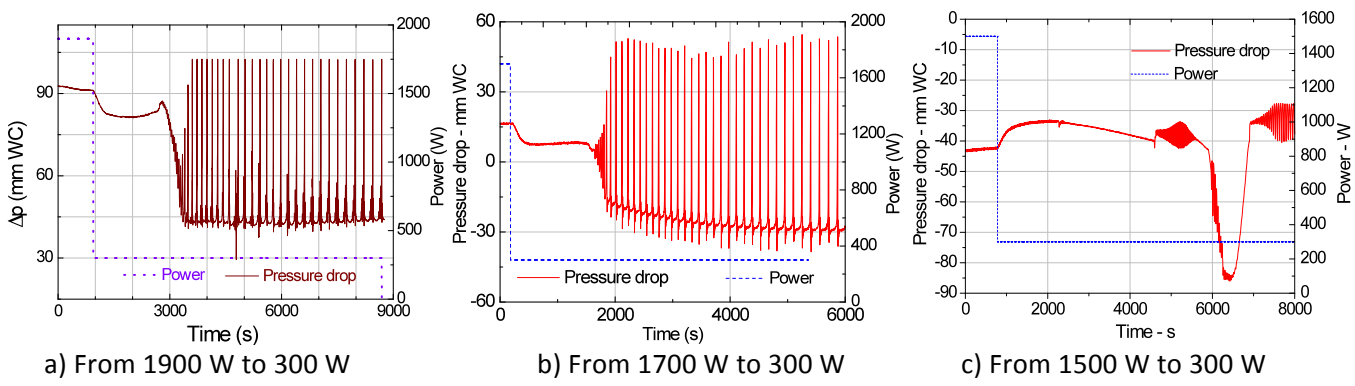
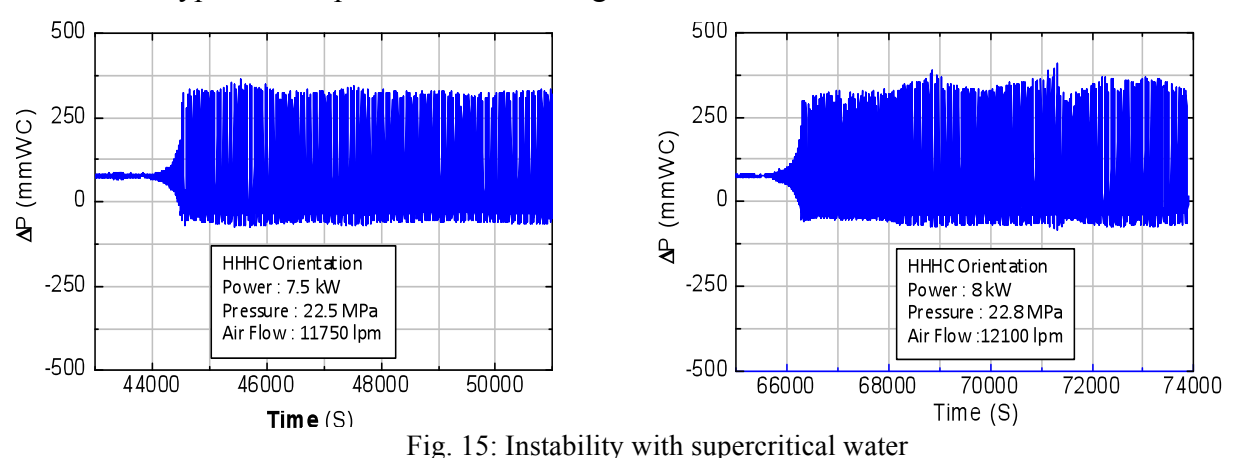


Fig. 14: Large power decrease from different initial powers

Instability with supercritical water

A stability investigation with water is on-going. Already a few cases of instability are observed with water. In all cases, the instability appeared in the pseudo-critical region with low coolant flow rates. Typical examples are shown in Fig. 15.



General Characteristics of the observed instability

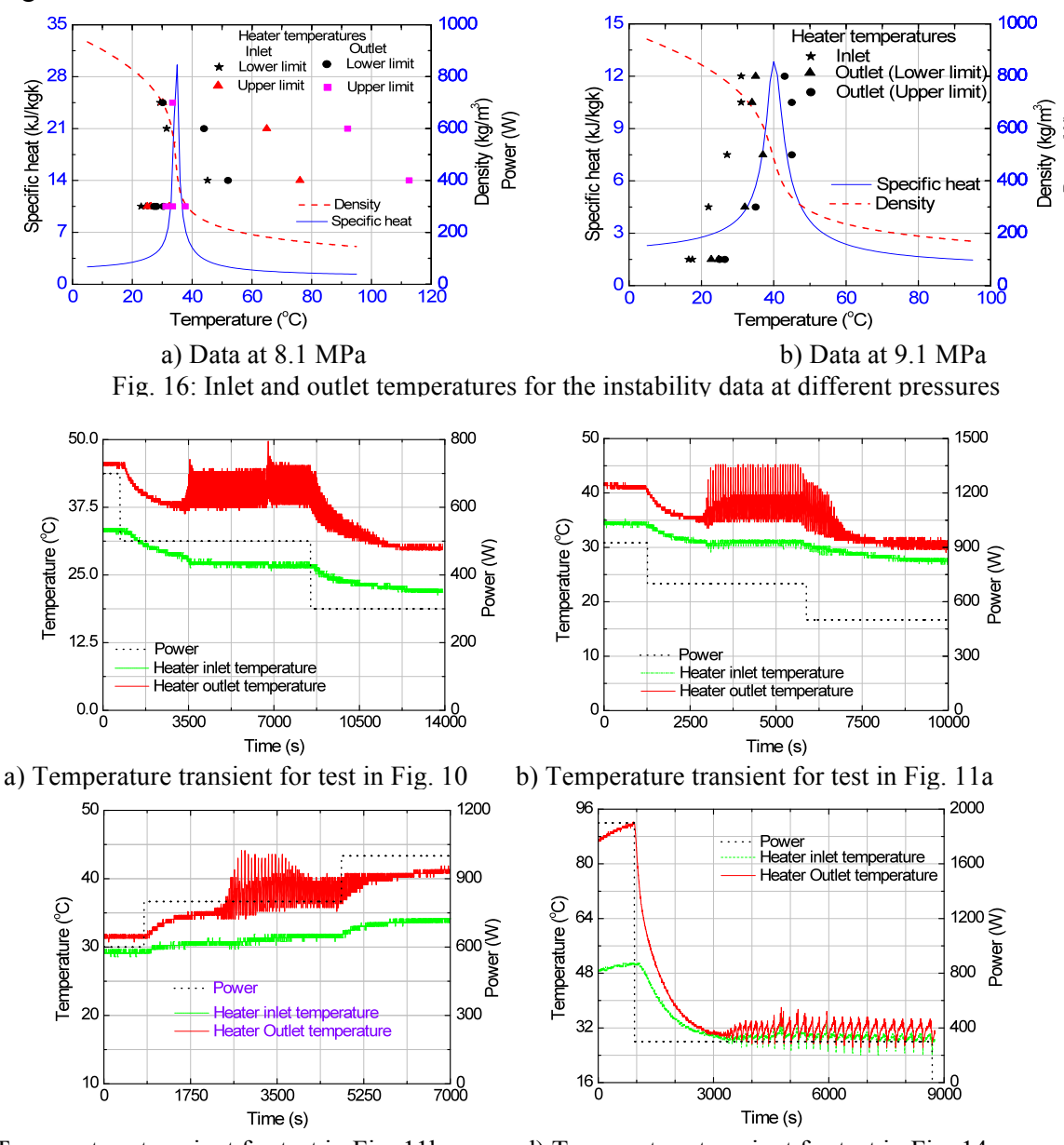
The amount of instability data generated in the present test facility is clearly inadequate compared to the extensive instability data that exists for single-phase and two-phase loops. The data generated is also inadequate to confirm certain characteristics of the instability like hysteresis though its existence is suspected. Further, the instability thresholds have not been successfully identified. Nevertheless several interesting characteristics have been revealed by the limited unstable data generated in the facility as brought out below.

Oscillatory Behaviour of Heater Inlet and Outlet temperatures

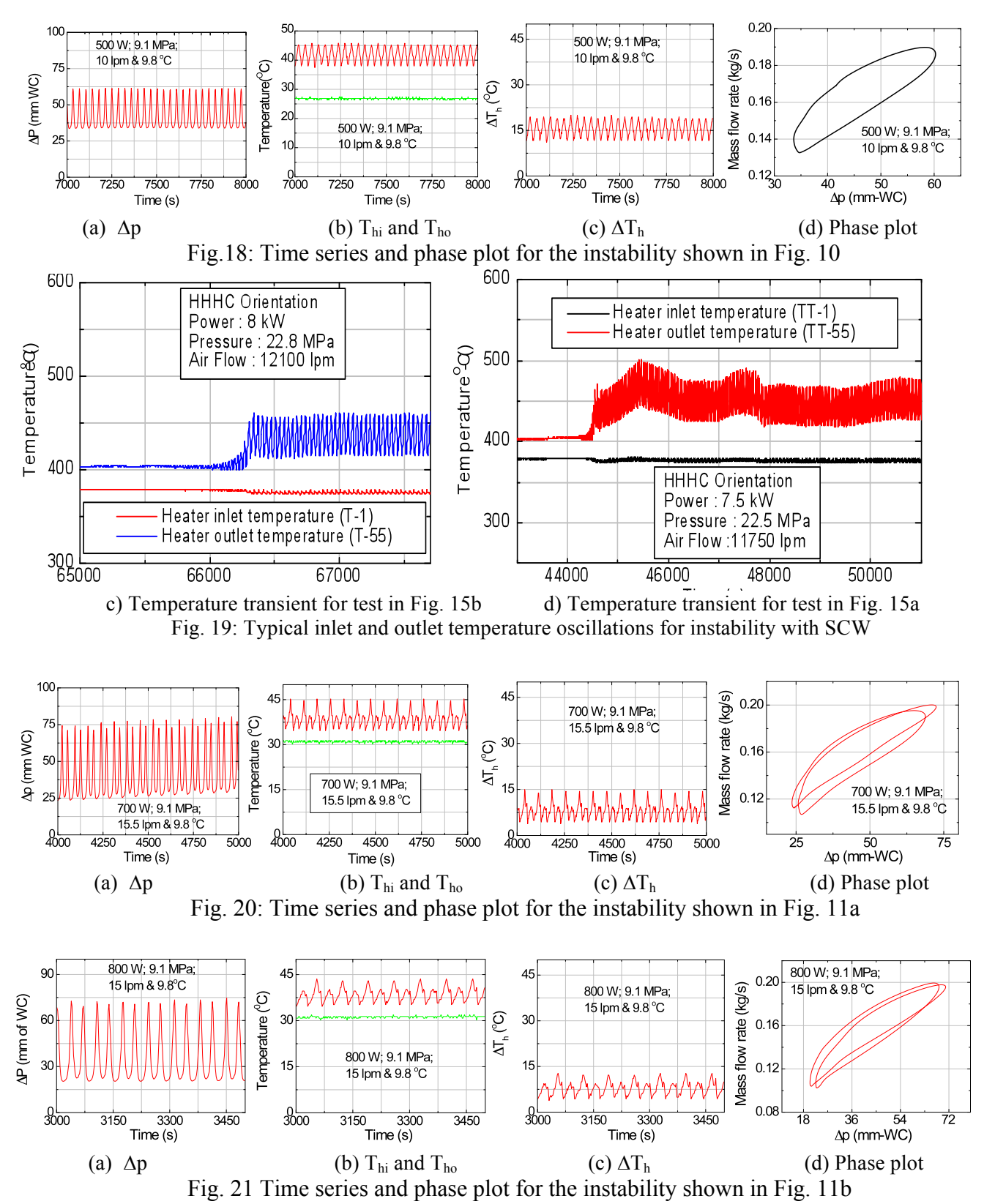
The minimum and maximum of the observed heater inlet and outlet temperature oscillations for all the CO₂ instability data at 8.1 and 9.1 MPa are shown in Fig. 16a and b respectively. Except

for the start-up at 400 W, all other instability data is found to be either in the pseudocritical region or close to it. Thus it appears that operation in or around the pseudocritical region is prone to instability for supercritical fluids. However, the start-up instability is not necessarily a characteristic of supercritical fluids. Instability during start-up has also been observed earlier for single-phase natural circulation loops [30]. Thus apart from the instability around the pseudocritical region, SPNCLs are also susceptible to other instability mechanisms of natural circulation.

Another interesting feature of the oscillations is that the inlet temperature remains almost constant and only outlet temperature is oscillating (see Fig. 17 & 18). This, however, is not the case with the instability observed with large power decrease as well as start-up (see also Fig. 17d). Fig. 19 confirms the same for water.



c) Temperature transient for test in Fig. 11b d) Temperature transient for test in Fig. 14a Fig. 17: Typical inlet and outlet temperature oscillations for instability at different powers



Time Series and Phase Plots

Analyses of the test data neglecting the initial transients often reveal many interesting characteristics of the instability. Figures 18, 20, 21 & 22 show the time series of measured Δp (pressure drop across the bottom horizontal pipe), T_{hi} & T_{ho} (inlet and outlet temperatures of the heater) and the ΔT_h (temperature rise across the heater) for one thousand seconds after neglecting the initial transients. As can be seen, the phase plot (shown for only one cycle) shows a simple closed curve for the test data at 500 W (see Fig. 18d) which is markedly different from that shown in figures 20d and 21d. From the time series given in Fig. 21 and 22, it is easily seen that a near period doubling occurs between 500 W and 700 W. In general, the period is expected to decrease with increase in power if the oscillatory mode remains the same. Switching of the oscillatory mode as shown by the phase plots results in sudden period change. Periodic oscillations depict a single closed phase plot. Both the oscillatory modes characterized by the phase plots in Fig. 18 and 20 or 21 are only nearly periodic as shown by the long duration phase plots in Fig. 22 and 23. Figures 22 and 23 also illustrates that the shape of the phase plots depends on the parameter spaces chosen (Lingade [31]).

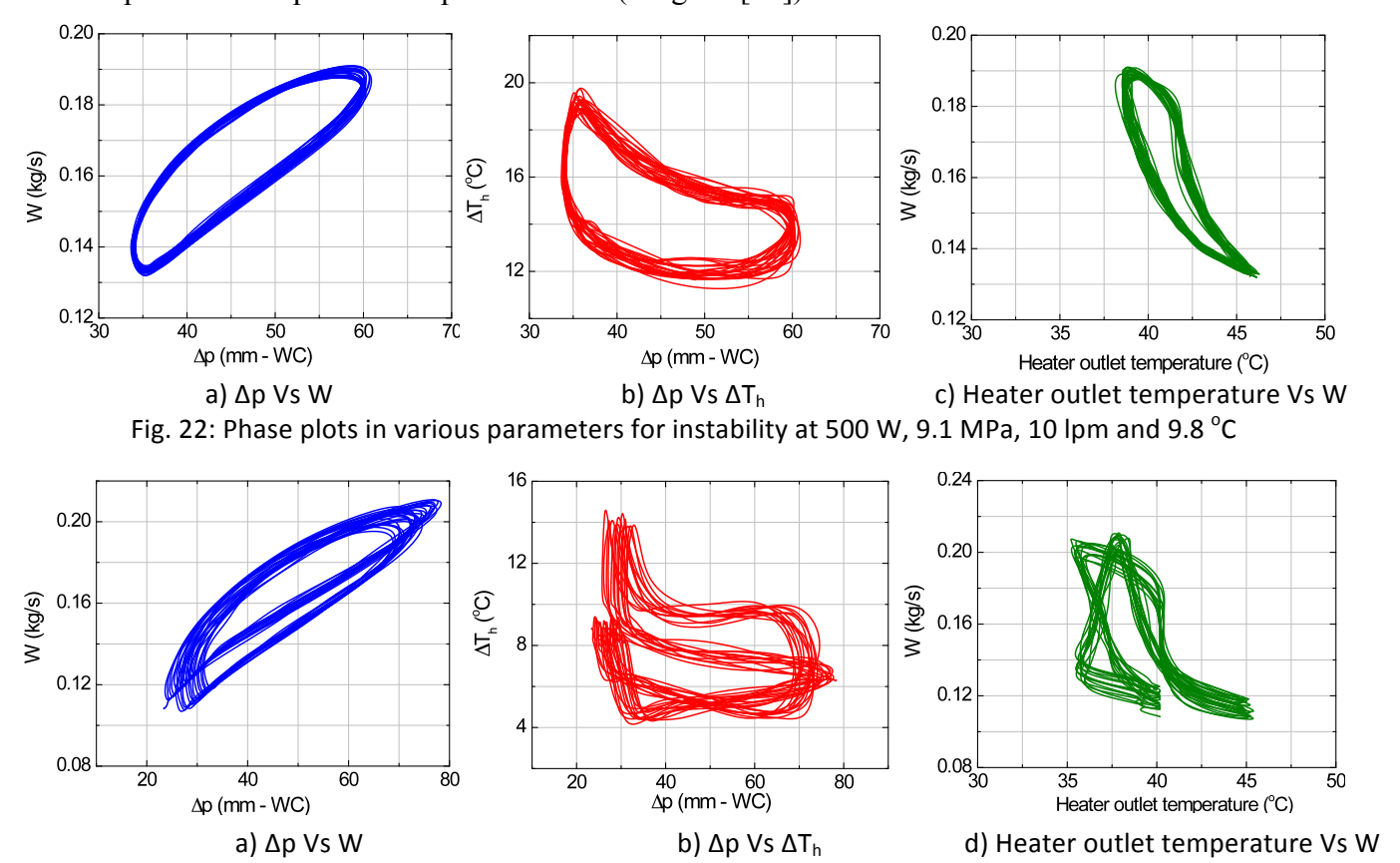


Fig. 23: Phase plots in various parameters for instability at 700 W, 9.1 MPa, 15.5 lpm and 9.8 °C

In the present experiments, instability with supercritical CO₂ and water was observed only at low coolant flow rates. Hence the effect of the secondary coolant flow rate on the stability of the CO₂ loop was studied with the nonlinear stability analysis code NOLSTA [25]. The code solves the 1-

D mass, momentum and energy conservation equations numerically in time domain. The code models the cooler with an overall heat transfer coefficient. Also, the pipes are considered adiabatic and their thermal capacitance effect is also neglected. The predicted stability map shows a lower and an upper instability threshold as observed in the experiments for a given secondary coolant mass flow rate as shown in Fig. 24. However, the predicted unstable zone is significantly larger than that was observed in the experiments. For example, no instability was observed beyond 30 lpm secondary flow rate during the experiments. This is attributed to the neglect of multi-dimensional effects, wall conduction and heat losses in the calculations.

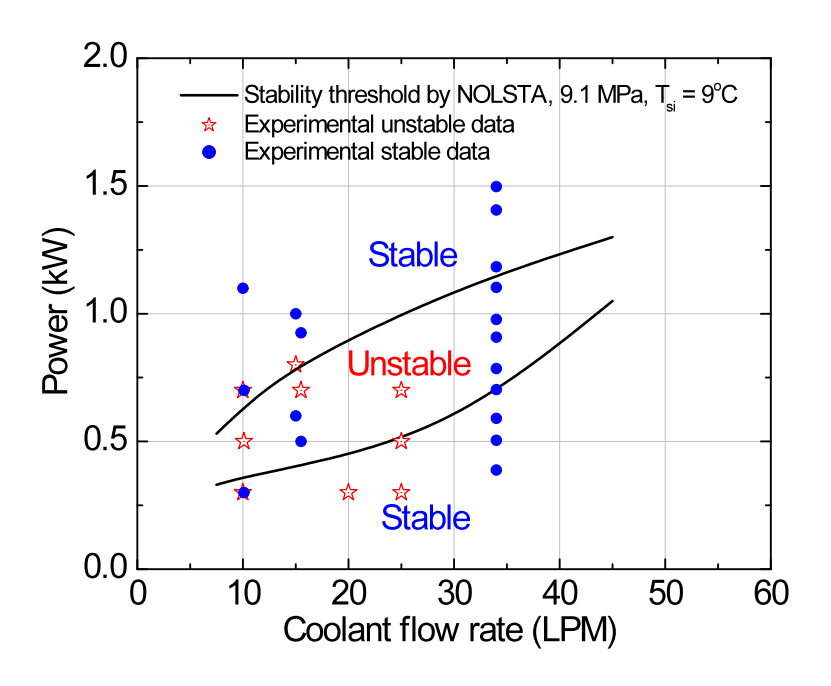


Fig.24: Effect of secondary coolant flow rate on the instability threshold

Concluding Remarks

Steady state and stability experiments were carried out with supercritical CO_2 and H_2O . The steady state flow rate data obtained were compared with the predictions of 1-D code NOLSTA which showed good agreement. The generalized steady state flow equation is able to predict the experimental flow rates within \pm 30%. Instability was observed in the loop in a narrow window around the pseudo critical region with low coolant flow rate for the HHHC orientation with both CO_2 and H_2O . One of the interesting feature of instability observed in most cases is that the heater outlet temperature is oscillating whereas heater inlet temperature is practically constant. All orientations of heater and cooler except HHHC were found to be stable over the range of parameters studied. NOLSTA code predicts a lower and an upper stability threshold which is in qualitative agreement with the experimental data.

Nomenclature

A Flow area (m^2)

D f g	Hydraulic diameter (m) Friction factor Acceleration due to gravity (m/s²)
Gr _m	Modified Grashoff Number, $\left[\frac{D^3 \rho_{pc} \rho_m \beta g Q_h H}{A \mu^3} \right]$
i	Enthalpy (j/kg/k)
Q_h	Heater Power (W)
Re	Reynolds number $(WD/A\mu)$
T	Temperature (°C)
W	Mass flow rate (kg/s)
Н	Loop height (m)

Greek

- ρ Density (kg/m³)
- β Volumetric expansion coefficient (k^{-1})
- μ Dynamic viscosity (Pa-s)

Subscripts

- h heater
- ho Heater outlet
- hi Heater inlet
- m mean
- pc Pseudo-critical
- si Secondary inlet

References

- 1) M.J. Driscoll & P. Hejzlar, 300 MWe Supercritical CO₂ Plant Layout and Design, Report No: MIT-GFR-014, MIT Nuclear Engineering Department, June 2004.
- 2) S.K.S. Tom and E.G. Hauptmann, The feasibility of cooling heavy water reactors with supercritical fluids, Nuclear Engineering and Design 53 (1979) 187-196.
- 3) J. Buongiorno and P.E. MacDonald, Supercritical water reactor (SCWR) Progress report for the FY-03 Generation-IV R&D activities for the development of the SCWR in the U.S., INEEL-EXT-03-01210, September 2003.
- 4) Y. Oka and S. Koshizuka, Supercritical pressure, once-through cycle light water cooled reactor concept, Journal of Nuclear Science & Technology, 38 (2001) 1081-89.
- 5) R.B. Duffey and K. Hedges, Future CANDU reactor development, ICONE-7459, ICONE-7, Tokyo, April 19-23, Tokyo, Japan, 1999.
- 6) J. Starflinger, N. Aksan, D. Bittermann, L. Heikinheimo, C. Maraczy, G. Rimpault, T. Schulenberg, Roadmap for Supercritical-Water-Cooled Reactor R&D in Europe, ICAPP'03 May 4-7, 2003, Cordoba, Spain.

- 7) V. Chatoorgoon, A. Voodi and D. Fraser, The stability boundary for supercritical flow in natural-convection loops Part I: H₂O studies, Nuclear Engineering and Design 235 (2005) 2570–2580.
- 8) T.O. Gomez, A. Class, R.T. Lahey Jr., and T. Schulenberg, Stability analysis of a uniformly heated channel with supercritical water, Nuclear Engineering and Design 239 (2009) 2952–2963.
- 9) V. Chatoorgoon, A. Voodi and P. Upadhyay, The stability boundary for supercritical flow in natural-convection loops Part II: CO₂ and H₂, Nuclear Engineering and Design 235 (2005) 2581–2593.
- 10) P.K. Jain, Rizwan-uddin, Numerical analysis of supercritical flow instabilities in a natural circulation loop, Nuclear Engineering and Design 238 (2008) 1947-1957.
- 11) L. Chen, Xin-Rong Zhang, H. Yamaguchi, Zhong-Sheng (Simon) Liu, Effect of heat transfer on instabilities and transitions of supercritical CO₂ flow in a natural circulation loop, International Journal of Heat and Mass Transfer 53 (2010) 4101-4111.
- 12) C.P. Marcel, M. Rhode, V.P. Masson and T.H.J.J. Van der Hagen, Fluid-to-fluid modeling of supercritical water loops for stability analysis, International Journal of Heat and Mass Transfer 52 (2009) 5046-5054.
- 13) M. Rhode, C.P. Marcel, C.T. Joen, A.G. Class and and T.H.J.J. Van der Hagen, Downscaling a supercritical water loop for experimental studies on system stability, International Journal of Heat and Mass Transfer 54 (2011) 65-74.
- 14) Walter Ambrosini, Discussion on the stability of heated channels with different fluids at supercritical pressures, Nuclear Engineering and Design 239 (2009) 2952–2963.
- 15) W. Ambrosini, M. Sharabi, Dimensionless parameters in stability analysis of heated channels with fluids at supercritical pressures, Nuclear Engineering and Design, 238(2008) 1917-1929.
- 16) Xin-Rong Zhang, L. Chen, H. Yamaguchi, Natural convective flow and heat transfer of supercritical CO2 in a natural circulation loop, International Journal of Heat and Mass Transfer 53 (2010) 4112-4122.
- 17) V.A. Silin, V.A. Voznesensky and A.M. Afrov, The light water integral reactor with natural circulation of the coolant at supercritical pressure BF-500 SKDI, Nuclear Engineering and Design 144 (1993) 327-336.
- 18) Bushby, S.J., Dimmick, G.R., Duffey, R.B., Spinks, N.J., Burrill, K.A. and Chan, P.S.W., Conceptual designs for advanced, high-temperature CANDU reactors, SCR-2000, Nov.6-8, 2000, Tokyo.
- 19) Lomperski, S., Cho, D., Jain, R., Corradini, M.L., 2004. Stability of a natural circulation loop with a fluid heated through the thermodynamic pseudocritical point. In: Proceedings of ICAPP '04, Pittsburgh, PA, USA, June 13–17, Paper 4268.
- 20) Harden, D.G., Transient behavior of a natural circulation loop operating near the thermodynamic critical point, ANL-6710, 1963.
- 21) Holman J.P and Boggs, J.H., Heat transfer to freon 12 near the critical state in a natural circulation loop, J. Heat Transfer 82 (1960) 221-226.
- 22) Yoshikawa, S., R.L. Smith Jr., H. Inomata, Y. Matsumura and K. Arai, Performance of a natural convection circulation system for supercritical fluids, J. of Supercritical Fluids 36 (2005) 70-80.

- 23) Zuber, N., 1966. An analysis of thermally induced flow oscillations in the near-critical and super-critical thermodynamic region, Report NASA-CR-80609, Research and Development Center, General Electric Company, Schenectady, NY, USA, May 25, 159 pp.
- 24) Vijayan P.K, Sharma, M, Pilkhwal D. S. and Saha D., Steady state and stability characteristics of a supercritical pressure natural circulation Loop (SPNCL) with CO₂, Annual Progress Report of the work done under IAEA Research Contract No. 14344/R2 as part of the IAEA CRP on Heat Transfer Behaviour and Thermo-Hydraulics Code Testing for SCWRs, 2010.
- 25) M. Sharma, P.K. Vijayan, D.S. Pilkhwal, D. Saha and R.K. Sinha, Linear and non-linear stability analysis of a supercritical natural circulation loop, ASME Journal of Engineering for Gas Turbines and Power, October 2010, Vol. 132 / 102904-1.
- 26) Swapnalee, B.T, Vijayan, P.K, Sharma, M, Pilkhwal, D.S. Saha, D. and Sinha, R.K, Steady state performance of subcritical and supercritical pressure natural circulation in the same test facility, ICONE-43232, accepted for the 19th International Conference on Nuclear Engineering, May 16-19, 2011, Chiba, Japan.
- 27) W. Ambrosini, and M.B. Sharabi, Assessment of stability maps for heated channels with supercritical fluids versus the predictions of a system code, Nuclear Engineering and Technology, Vol.39, 627-636, 2007.
- 28) W. Ambrosini, M. B. Sharabi, Dimensionless parameters in stability analysis of heated channels with fluids at supercritical pressures, Nuclear Engineering and Design, 238 (2008) 1917-1929.
- 29) Welander, P., On the oscillatory instability of a differentially heated loop, J. Fluid Mech. (1967) 29 17-30.
- 30) P.K. Vijayan, A.K. Nayak, D. Saha and M.R.Gartia, Effect of loop diameter on the steady state and stability behaviour of single-phase and two-phase natural circulation loops, Science and Technology of Nuclear Installations, Vol. 2008, Article ID 672704.
- 31) B.M. Lingade, Heat transfer and stability studies on supercritical natural circulation loop, M.Tech. thesis, 2010, Homi Bhabha National Institute, Mumbai 400094, India.